THE GEOLOGICAL SOCIETY OF AMERICA®

The transitional climate of the late Miocene Arctic: Winter-dominated precipitation with high seasonal variability

Brian A. Schubert[1], A. Hope Jahren[2], Sergei P. Davydov[3], and Sophie Warny[4]
[1]School of Geosciences, University of Louisiana at Lafayette, Lafayette, Louisiana 70504, USA
[2]Centre for Earth Evolution and Dynamics, University of Oslo, N-0315 Oslo, Norway
[3]North-East Science Station, Far East Branch of Russian Academy of Sciences, Cherskiy, Russia
[4]Department of Geology and Geophysics and Museum of Natural Science, Louisiana State University, Baton Rouge, Louisiana 70803, USA

ABSTRACT

The late Miocene (11.6–5.3 Ma) was an important transitional period following the greenhouse conditions of the Eocene. In order to gain insight into the Arctic paleoclimate of the time, we performed high-resolution intraring $\delta^{13}C$ analyses on fossil wood collected from the late Miocene Khapchansky sediments of northeastern Siberia (~69°N). From these data we quantified the ratio of summer to winter precipitation (P_s/P_w) and compared it to current values for the region determined from modern wood samples and instrumental records. We observed much greater frequency of winter-dominated precipitation ($P_s/P_w < 1$) and much greater variability in P_s/P_w during the Miocene than today. Specifically, years with $P_s/P_w < 1$ occurred three times more often, and years with at least three times as much precipitation in summer or winter ($0.33 < P_s/P_w < 3.0$) occurred approximately twice as often during the Miocene than today. We attribute the high interannual variability in precipitation to an inconsistent moisture source associated with the relatively unstable and incomplete ice cover in the Arctic Ocean during the late Miocene. Our result highlights the potential for enhanced variability in Arctic precipitation in response to Arctic sea ice decline caused by anthropogenic, CO_2-induced warming.

INTRODUCTION

Eastern Siberia (a 7.3×10^6 km^2 area, similar to Australia in size) features numerous plant fossil localities (e.g., Baekovo and Nekkeiveem, Khapchan-Timmerdekh, Mamontova Gora), many with exceptionally preserved Neogene fossils (e.g., Baranova and Grinenko, 1989; Baranova et al., 1970; Dorofeev, 1969; Grinenko et al., 1989; Nikitin, 2007). The Miocene (23–5.3 Ma) is particularly well represented within the sediments of eastern Siberia (Gnibidenko et al., 2011; Nikitin, 2007; Volkova and Kul'kova, 1996; Volkova et al., 1986). This period represents a notable time characterized by global cooling (with the exception of the Middle Miocene Climatic Optimum) following the greenhouse conditions of the Paleogene (Zachos et al., 2008); however, the Arctic hydrology is poorly constrained. We hypothesize year-to-year variability in seasonal precipitation increased in the Arctic during the late Miocene as a result of unstable and intermittent sea ice cover (Darby, 2014; Stein et al., 2016). To test this, we present a reconstruction of seasonal precipitation at annual resolution for the late Miocene using high-resolution $\delta^{13}C$ measurements across fossil growth rings, thus producing the first interannual paleoclimate record for the Siberian Arctic. Resolution of year-to-year changes in seasonal precipitation represents a critical advance beyond the reconstruction of mean annual conditions, particularly in assessing the influence of climate on vegetation. Within modern environments, the timing and amount of seasonal precipitation have been shown to exert a strong influence on net primary productivity (Robertson et al., 2009), ecosystem respiration (Chimner and Welker, 2005), and species diversity and abundances (Robertson et al., 2010). Within Arctic environments specifically, winter precipitation (including snowfall and snowmelt) has been shown to affect the distribution of plant species (Beck et al., 2005), net ecosystem production (Uchida et al., 2010), and the length of growing seasons (Ernakovich et al., 2014). For these reasons, we sought to quantify the seasonal variability of precipitation during the late Miocene, and discuss the effect of ice cover in the Arctic Ocean on precipitation and Arctic vegetation, as characterized by the fossil record.

MATERIALS AND METHODS

We collected mummified fossil wood from the Finish Stream site (68.724°N, 161.587°E) located near the Cherskiy Field Station in eastern Siberia (Sakha Republic, Russia; Fig. 1A). Wood samples as much as 10 cm in length and 3 cm in diameter were excavated from the late Miocene Khapchansky horizon (Fig. DR1 in the GSA Data Repository[1]). In order to refine the age context of the Finish Stream site, a palynology analysis was performed (see the Data Repository). Six mummified wood pieces were sampled using a razor blade parallel to the growth rings for intraring $\delta^{13}C$ analysis (for methods, see our previous studies on modern and fossil wood: Jahren and Sternberg, 2008; Schubert and Jahren, 2011, 2015; Schubert et al., 2012; Schubert and Timmermann, 2015; see the Data Repository).

In order to contrast the results of our paleoclimate analysis using fossil wood against an analysis of modern wood collected from the same site, we sampled wood from two living *Pinus pumila* (dwarf Siberian pine; PINE01 and PINE02) growing at the Cherskiy site (Fig. DR2), using the same methods (see the Data Repository). These plants were chosen due to their similarity to the *Pinus* wood fragments identified within the late Miocene Khapchansky horizon (Grinenko et al., 1997). The modern wood samples ranged from ~3 to 4 cm in diameter and showed clear annual growth rings (Fig. DR2).

RESULTS

When we examined the isotope data gained from the analysis of modern *Pinus* wood growing at the Cherskiy site, we found that both samples showed similar intraring $\delta^{13}C$ patterns (Fig. 2A), but that sample PINE01 had a significantly ($p < 0.0001$) higher $\delta^{13}C$ value ($\delta^{13}C = -27.4‰ \pm 0.6‰$, $n = 107$) than PINE02 ($\delta^{13}C = -28.1‰ \pm 0.5‰$, $n = 148$). The total range of $\delta^{13}C$ values in the modern wood, however, was small (−29.4‰ to −26.3‰). In contrast, we observed a wide range in $\delta^{13}C$ values for the fossil wood (−27.2‰ to −20.8‰), resulting from the larger number of samples analyzed; however, each showed a similar intra-annual $\delta^{13}C$

[1]GSA Data Repository item 2017133, supplementary information on the stratigraphic context and palynology analysis, stable isotope methods, and photographs of the field site and collected specimens, is available online at http://www.geosociety.org/datarepository/2017/ or on request from editing@geosociety.org.

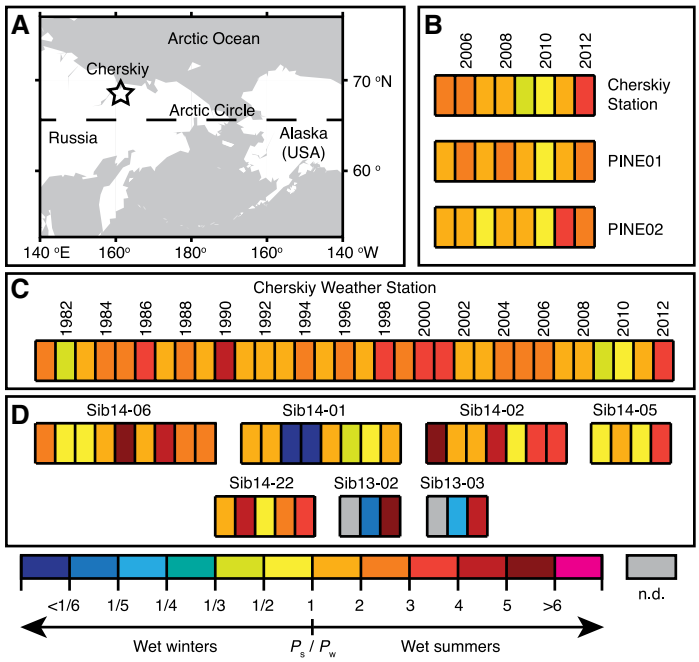

Figure 1. Seasonal precipitation, measured as the ratio of summer (P_s: May through October) to winter (P_w: November through April) precipitation. Each colored rectangle represents one year. A: Location of modern and fossil wood samples collected near Cherskiy, Russia (star). B: Comparison of year-to-year changes in P_s/P_w measured at the Cherskiy weather station to those determined from high-resolution $\delta^{13}C$ measurements across two modern *Pinus pumila* plants (PINE01, PINE02). C: Long-term record of P_s/P_w measured at the Cherskiy weather station. D: Late Miocene P_s/P_w determined from high-resolution $\delta^{13}C$ measurements across six pieces of fossil wood. Interannual changes in P_s/P_w determined from modern growth rings are consistent with the local weather station (B), but show much less variability than values determined for the late Miocene using fossil wood (D). This contrasts with the low variability in P_s/P_w determined for the Arctic Eocene (Schubert et al., 2012). The gray box (labeled n.d.) indicates that P_s/P_w could not be determined ($\delta^{13}C_{max}$ occurred at the start of the profile and therefore $\delta^{13}C_{min}$ was not present).

pattern (Fig. 2B) consistent with modern and fossil evergreen wood, as observed in wood from around the world (Schubert and Jahren, 2011; Schubert et al., 2012). The fossil wood sample Sib13, measured across two different radii, showed excellent intrasample reproducibility in the $\delta^{13}C$ pattern (Fig. 2A), suggesting that the radius sampled does not affect the $\delta^{13}C$ pattern, consistent with previous studies on other species (e.g., Verheyden et al., 2004).

The intra-annual $\delta^{13}C$ pattern within the mummified fossil wood has previously been used to reconstruct the ratio of summer (P_s) to winter (P_w) precipitation for the site at which the plant grew (Schubert et al., 2012; Schubert and Timmermann, 2015), using the following equation derived from patterns seen in 33 modern angiosperms and gymnosperms growing across a wide range of environments (including high latitude), totaling 15 sites (Schubert and Jahren, 2011):

$$P_s/P_w = e^{\wedge}\left\{\left[\Delta\left(\delta^{13}C\right) - (0.01L + 0.13) - 0.73\right]/-0.82\right\}, \quad (1)$$

where L is latitude, e is a mathematical constant (~2.718), and $\Delta(\delta^{13}C)$ is calculated as the difference between the maximum $\delta^{13}C$ value of a given year ($\delta^{13}C_{max}$) and the preceding minimum $\delta^{13}C$ value of the annual cycle ($\delta^{13}C_{min}$) [$\Delta(\delta^{13}C) = \delta^{13}C_{max} - \delta^{13}C_{min}$].

We compared values of P_s/P_w calculated, according to Equation 1, from high-resolution $\delta^{13}C$ analysis across modern wood of *P. pumila* growing at the Cherskiy site with the actual climate conditions, as recorded in terms

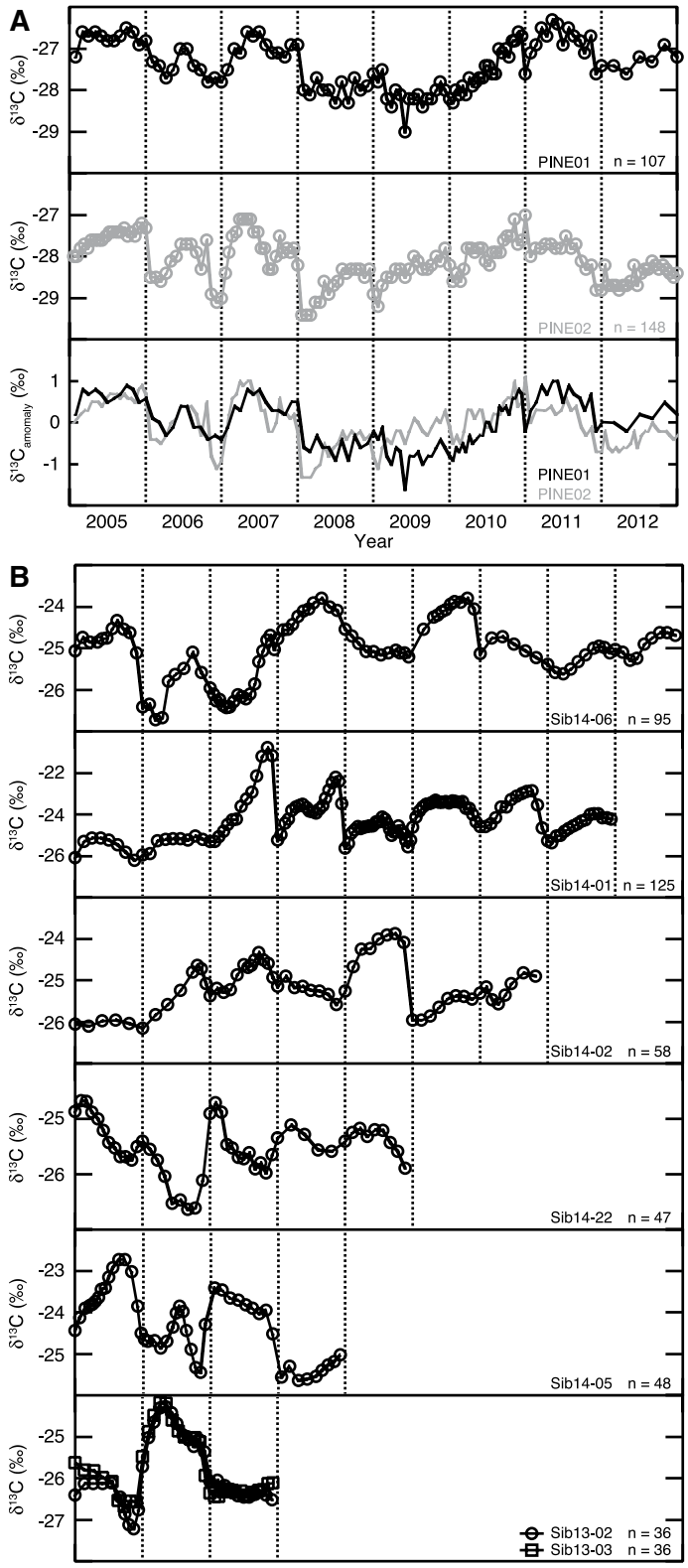

Figure 2. High-resolution $\delta^{13}C$ measurements across annual growth rings. Vertical dashed lines mark ring boundaries; growth is from left to right. A: Modern *Pinus pumila* wood. Although $\delta^{13}C$ values measured within PINE01 were significantly higher than in PINE02, the relative changes in $\delta^{13}C$ ($\delta^{13}C_{anomaly}$) were consistent between both samples. B: Late Miocene wood. The $\delta^{13}C$ pattern of each fossil suggests that the plants represent evergreen (rather than deciduous) species (Helle and Schleser, 2004; Schubert and Jahren, 2011), and are therefore consistent with the *Pinus* wood fragments previously identified within this horizon (Grinenko et al., 1997).

of seasonal precipitation. Across eight consecutive years (2005–2012), our calculated P_s/P_w values agreed well with P_s/P_w values determined from a local weather station (Fig. 1B); specifically, the average P_s/P_w determined from the intra-annual $\delta^{13}C$ data ($P_s/P_w = 1.75 \pm 0.53$, n = 8) was not significantly different (p = 0.85) from data collected at the local weather station ($P_s/P_w = 1.67 \pm 0.84$, n = 8). When expanding our examination of the climate at this site across the entirety of its record (n = 32 yr; 1981–2012), we saw that the site consistently had a summer-dominated precipitation regime, with more than 90% of the years between 1981 and 2012 exhibiting greater precipitation during summer than during winter (Fig. 1C).

In order to test whether this summer-dominated precipitation regime also existed in the Arctic during the time when our fossil plants were growing (i.e., the late Miocene), we performed high-resolution $\delta^{13}C$ analyses across 36 fossil growth rings taken from 6 different mummified wood fossils (Fig. 2B). From these data we reconstructed P_s/P_w values for each year of growth using Equation 1 (Fig. 1D).

The year-to-year variability in P_s/P_w calculated for the late Miocene using Equation 1 (Fig. 1D) is striking compared with the lack of year-to-year variability evidenced within the modern climate record at the site (Fig. 1C), and as reflected by modern wood growing at the site (Fig. 1B). Nearly one-third of the late Miocene $\delta^{13}C$ profiles within rings (11 out of 36 yr) indicated a winter-dominated precipitation regime, compared to only 3 of 32 yr within the modern extended record. In addition, according to the reconstructed late Miocene data set, extreme seasonal variability (defined as years with at least 3× more precipitation during summer, or during winter; i.e., $0.33 < P_s/P_w < 3.0$) was approximately twice as common compared to today.

DISCUSSION

The P_s/P_w values reconstructed for northeastern Siberia during the late Miocene indicate that the summer-dominated precipitation regime characteristic of the modern Arctic (New et al., 2002) was not a stable feature throughout the Neogene. At present, the very low temperatures found across the continental regions of the Arctic preclude the presence of significant water vapor within the atmosphere during winter, resulting in a consistently summer-dominated pattern in annual precipitation (Fig. 1C).

Using the Yanran flora, Popova et al. (2012) reconstructed both cold month mean temperature (CMMT) and mean annual precipitation (MAP) for a site in northeastern Siberia, located <100 km from the Cherskiy site and dated to be late Miocene. Popova et al. (2012) determined the CMMT to have been −3 °C, much higher than today's CMMT at Cherskiy (−35 °C). This higher temperature during the late Miocene could have allowed for substantially more atmospheric water vapor relative to today (e.g., Higgins and Cassano 2009); Popova et al. (2012) reconstructed the MAP to 581–1206 mm, similar to London, UK (602 mm) or New York City, USA (1200 mm), and much higher than today's MAP at Cherskiy (233 mm).

The extreme seasonal variability in precipitation patterns reconstructed here for the late Miocene (Fig. 1D) was contemporaneous with the onset of Arctic sea ice (Lavrushin and Alekseev, 2005). The first formation of ice within the Arctic Ocean represented the culmination of long-term and global-scale cooling driven by a decline in atmospheric CO_2 levels that began during the Eocene (Zachos et al., 2008) and extended into the late Miocene (Herbert et al., 2016). The perennial ice cover in the central Arctic Ocean observed today was lacking, at least intermittently (Darby, 2014), during the late Miocene (Stein et al., 2016).

This relatively unstable and incomplete ice cover during the late Miocene likely resulted in high interannual variations in evaporation of water from the Arctic Ocean that we observed in the high interannual precipitation variability signal of our data (Fig. 1D). This climate configuration likely persisted until the Pliocene, by which time this region began forming permafrost sediments (Sher et al., 1979) and the entire Eurasian sector of the Arctic Ocean was fully ice-covered (Knies et al., 2014). Thus, the late Miocene represented a transitional period for Arctic climate, i.e., much cooler and more seasonally variable than the consistently summer-precipitation greenhouse conditions of the Eocene (Jahren and Sternberg, 2003; Schubert et al., 2012), but not yet ice-locked into the colder winters of the Pliocene (Popova et al., 2012). We attribute the greater precipitation seasonality in the Arctic during the late Miocene to the onset of intermittent Arctic sea ice.

The unique transitional climate conditions of the late Miocene were also associated with a shift from forest cover to more open landscapes in the Siberian Arctic (Popova et al., 2013). Pollen extracted from sediments at the Cherskiy site corroborated these claims, and indicated an environment dominated by shrubs and microplants, rather than trees, during the late Miocene; the lack of any report of large wood fragments within the Khapchansky horizon was also consistent with more limited biomass in this region during the late Miocene, and with the aridification of both western and eastern Siberia (Miao et al., 2012). The wood pieces we collected from the Finish Stream site were small (<10 cm in length, <3 cm in diameter) (Fig. DR1), in contrast to the very large wood pieces and stumps identified in the Arctic during the Eocene (e.g., Jahren, 2007) and middle Miocene (Williams et al., 2008).

CONCLUSIONS

The high variability in $\Delta(\delta^{13}C)$ determined for fossil wood of late Miocene age from northeastern Siberia is in stark contrast to that measured within growth rings sampled from modern wood collected at the site. Our data suggest that the Arctic site had a mix of summer- and winter-dominated precipitation regimes during the late Miocene, and that high year-to-year variability in the timing of maximum precipitation was common. This seasonal variability, combined with the unique light regime of the Arctic, likely had a governing influence in limiting the plant biomass found represented in the fossil record of the region. Taken together, our results highlight the important role of winter temperatures and the presence of sea ice in regulating precipitation delivery and the resulting plant biomass in the Arctic during the late Miocene.

High variability in seasonal precipitation could therefore return to Arctic regions as a result of high-latitude warming driven by increasing atmospheric CO_2. Models and observational data suggest that increased heavy precipitation events occur in response to higher temperatures (Fischer and Knutti, 2015). Sea ice affects the Arctic hydrologic cycle by altering large-scale atmospheric circulation patterns and the amount of evaporation and precipitation (Kopec et al., 2016). As sea ice declines, models predict that precipitation will increase, especially in winter months, as a result of enhanced warming, water vapor, and evaporation; decreases in sea-level pressure; and an increase in convective and low cloud cover (Deser et al., 2010; Singarayer et al., 2006). It therefore follows that more intermittent sea ice as a result of global warming may lead to more variability in the source and timing of precipitation in the coming decades. Our work illustrates how seasonally variable precipitation regimes have significant ramifications for primary productivity within Arctic regions.

ACKNOWLEDGMENTS

We thank W.M. Hagopian for field and laboratory assistance; Y. Xu and M.W. Trahan for laboratory assistance; N. Zimov and S. Zimov for field assistance; and R.G.M. Spencer, E. Bulygina, and R.M. Holmes for logistical support. This work was supported by NSF grants EAR-MA130015 (Schubert) and EAR-1250063 (Jahren), and the Research Council of Norway through its Centers of Excellence funding scheme #223272 (Jahren).

REFERENCES CITED

Baranova, Y.P., and Grinenko, O.V., eds., 1989, Paleogene and Neogene strata of the northeastern USSR: USSR Academy of Science, Siberian Branch, Yakut Institute of Geological Sciences, Yakut Scientific Center, 182 p. (in Russian).

Baranova, Y.P., Kul'kova, I.A., Nikitin, V.P., and Shvareva, N.Y., 1970, New data on Miocene deposits of Mamontova Gora on the Aldan River: USSR Academy of Sciences Proceedings, v. 193, p. 1119–1122.

Beck, P.S.A., Kalmbach, E., Joly, D., Stien, A., and Nilsen, L., 2005, Modelling local distribution of an Arctic dwarf shrub indicates an important role for remote

sensing of snow cover: Remote Sensing of Environment, v. 98, p. 110–121, doi:10.1016/j.rse.2005.07.002.
Chimner, R.A., and Welker, J.M., 2005, Ecosystem respiration responses to experimental manipulations of winter and summer precipitation in a mixedgrass prairie, WY, USA: Biogeochemistry, v. 73, p. 257–270, doi:10.1007/s10533-004-1989-6.
Darby, D.A., 2014, Ephemeral formation of perennial sea ice in the Arctic Ocean during the middle Eocene: Nature Geoscience, v. 7, p. 210–213, doi:10.1038/ngeo2068.
Deser, C., Tomas, R., Alexander, M., and Lawrence, D., 2010, The seasonal atmospheric response to projected Arctic sea ice loss in the late twenty-first century: Journal of Climate, v. 23, p. 333–351, doi:10.1175/2009JCLI3053.1.
Dorofeev, P.I., 1969, The Miocene flora of Mammoth Mountain on the Aldan River: Leningrad, V.L. Komarov Botanical Institute, Academia Nauka SSSR (in Russian with English summary).
Ernakovich, J.G., Hopping, K.A., Berdanier, A.B., Simpson, R.T., Kachergis, E.J., Steltzer, H., and Wallenstein, M.D., 2014, Predicted responses of arctic and alpine ecosystems to altered seasonality under climate change: Global Change Biology, v. 20, p. 3256–3269, doi:10.1111/gcb.12568.
Fischer, E.M., and Knutti, R., 2015, Anthropogenic contribution to global occurrence of heavy-precipitation and high-temperature extremes: Nature Climate Change, v. 5, p. 560–564, doi:10.1038/nclimate2617.
Gnibidenko, Z.N., Volkova, V.S., Kuz'mina, O.B., Dolya, Z.A., Khazina, I.V., and Levicheva, A.V., 2011, Stratigraphic, paleomagnetic, and palynological data on the Paleogene–Neogene continental sediments of southwestern West Siberia: Russian Geology and Geophysics, v. 52, p. 466–473, doi:10.1016/j.rgg.2011.1003.1009.
Grinenko, O.V., Sergenko, A.I., and Belolyubsky, I.N., 1989, Paleogene and Neogene strata of the northeastern USSR. Part I. Regional stratigraphic chart of Paleogene and Neogene deposits of northeastern Russia and explanatory note (in Russian).
Grinenko, O.V., Sergenko, A.I., and Belolyubsky, I.N., 1997, Stratigraphy of the Paleogene and Neogene sediments of north east Russia: Otechestvennaya Geologiya, v. 8, p. 14–20 (in Russian).
Helle, G., and Schleser, G.H., 2004, Beyond CO_2-fixation by Rubisco—An interpretation of $^{13}C/^{12}C$ variations in tree rings from novel intra-seasonal studies on broad-leaf trees: Plant, Cell & Environment, v. 27, p. 367–380, doi:10.1111/j.0016-8025.2003.01159.x.
Herbert, T.D., Lawrence, K.T., Tzanova, A., Peterson, L.C., Caballero-Gill, R., and Kelly, C.S., 2016, Late Miocene global cooling and the rise of modern ecosystems: Nature Geoscience, v. 9, p. 843–847, doi:10.1038/ngeo2813.
Higgins, M.E., and Cassano, J.J., 2009, Impacts of reduced sea ice on winter Arctic atmospheric circulation, precipitation, and temperature: Journal of Geophysical Research, v. 114, D16107, doi:10.1029/2009JD011884.
Jahren, A.H., 2007, The Arctic forest of the middle Eocene: Annual Review of Earth and Planetary Sciences, v. 35, p. 509–540, doi:10.1146/annurev.earth.35.031306.140125.
Jahren, A.H., and Sternberg, L.S.L., 2003, Humidity estimate for the middle Eocene Arctic rain forest: Geology, v. 31, p. 463–466, doi:10.1130/0091-7613(2003)031<0463:HEFTME>2.0.CO;2.
Jahren, A.H., and Sternberg, L.S.L., 2008, Annual patterns within tree rings of the Arctic middle Eocene (ca. 45 Ma): Isotopic signatures of precipitation, relative humidity, and deciduousness: Geology, v. 36, p. 99–102, doi:10.1130/G23876A.1.
Knies, J., Cabedo-Sanz, P., Belt, S.T., Baranwal, S., Fietz, S., and Rosell-Melé, A., 2014, The emergence of modern sea ice cover in the Arctic Ocean: Nature Communications, v. 5, 5608, doi:10.1038/ncomms6608.
Kopec, B.G., Feng, X., Michel, F.A., and Posmentier, E.S., 2016, Influence of sea ice on Arctic precipitation: Proceedings of the National Academy of Sciences of the United States of America, v. 113, p. 46–51, doi:10.1073/pnas.1504633113.
Lavrushin, Y.A., and Alekseev, M.N., 2005, The arctic regions, *in* Velichko, A.A., and Nechaev, V.P., eds., Cenozoic climatic and environmental changes in Russia: Geological Society of America Special Paper 382, p. 13–29, doi:10.1130/0-8137-2382-5.13.
Miao, Y., Herrmann, M., Wu, F., Yan, X., and Yang, S., 2012, What controlled Mid–Late Miocene long-term aridification in Central Asia?—Global cooling or Tibetan Plateau uplift: A review: Earth-Science Reviews, v. 112, p. 155–172.
New, M., Lister, D., Hulme, M., and Makin, I., 2002, A high-resolution data set of surface climate over global land areas: Climate Research, v. 21, p. 1–25, doi:10.3354/cr021001.
Nikitin, V.P., 2007, Paleogene and Neogene strata in northeastern Asia: Paleocarpological background: Russian Geology and Geophysics, v. 48, p. 675–682, doi:10.1016/j.rgg.2006.06.002.
Popova, S., Utescher, T., Gromyko, D., Bruch, A.A., and Mosbrugger, V., 2012, Palaeoclimate evolution in Siberia and the Russian Far East from the Oligocene to Pliocene—Evidence from fruit and seed floras: Turkish Journal of Earth Sciences, v. 21, p. 315–334, doi:10.3906/yer-1005-6.
Popova, S., Utescher, T., Gromyko, D.V., Mosbrugger, V., Herzog, E., and François, L., 2013, Vegetation change in Siberia and the northeast of Russia during the Cenozoic cooling: A study based on the diversity of plant funcational types: Palaios, v. 28, p. 418–432, doi:10.2110/palo.2012.p12-096r.
Robertson, T.R., Bell, C.W., Zak, J.C., and Tissue, D.T., 2009, Precipitation timing and magnitude differentially affect aboveground annual net primary productivity in three perennial species in a Chihuahuan Desert grassland: New Phytologist, v. 181, p. 230–242, doi:10.1111/j.1469-8137.2008.02643.x.
Robertson, T.R., Zak, J.C., and Tissue, D.T., 2010, Precipitation magnitude and timing differentially affect species richness and plant density in the sotol grassland of the Chihuahuan Desert: Oecologia, v. 162, p. 185–197, doi:10.1007/s00442-009-1449-z.
Schubert, B.A., and Jahren, A.H., 2011, Quantifying seasonal precipitation using high-resolution carbon isotope analyses in evergreen wood: Geochimica et Cosmochimica Acta, v. 75, p. 7291–7303, doi:10.1016/j.gca.2011.7208.7002.
Schubert, B.A., and Jahren, A.H., 2015, Seasonal temperature and precipitation recorded in the intra-annual oxygen isotope pattern of meteoric water and tree-ring cellulose: Quaternary Science Reviews, v. 125, p. 1–14, doi:10.1016/j.quascirev.2015.07.024.
Schubert, B.A., and Timmermann, A., 2015, Reconstruction of seasonal precipitation in Hawai'i using high-resolution carbon isotope measurements across tree rings: Chemical Geology, v. 417, p. 273–278, doi:10.1016/j.chemgeo.2015.10.013.
Schubert, B.A., Jahren, A.H., Eberle, J.J., Sternberg, L.S.L., and Eberth, D.A., 2012, A summertime rainy season in the Arctic forests of the Eocene: Geology, v. 40, p. 523–526, doi:10.1130/G32856.1.
Sher, A.V., Kaplina, T.N., Giterman, R.E., Lozhkin, A.V., Arkhangelov, A.A., Kiselyov, S.V., Kouznetsov, Y.V., Virina, E.I., and Zazhigin, V.S., 1979, Late Cenozoic of the Kolyma Lowland: XIV Pacific Science Congress, Tour Guide XI, Khabarovsk August 1979: Moscow, USSR Academy of Sciences, p. 1–116.
Singarayer, J.S., Bamber, J.L., and Valdes, P.J., 2006, Twenty-first-century climate impacts from a declining Arctic sea ice cover: Journal of Climate, v. 19, p. 1109–1125, doi:10.1175/JCLI3649.1.
Stein, R., et al., 2016, Evidence for ice-free summers in the late Miocene central Arctic Ocean: Nature Communications, v. 7, 11148, doi:10.1038/ncomms11148.
Uchida, M., Kishimoto, A., Muraoka, H., Nakatsubo, T., Kanda, H., and Koizumi, H., 2010, Seasonal shift in factors controlling net ecosystem production in a high Arctic terrestrial ecosystem: Journal of Plant Research, v. 123, p. 79–85, doi:10.1007/s10265-009-0260-6.
Verheyden, A., Helle, G., Schleser, G.H., Dehairs, F., Beeckman, H., and Koedam, N., 2004, Annual cyclicity in high-resolution stable carbon and oxygen isotope ratios in the wood of the mangrove tree *Rhizophora mucronata*: Plant, Cell & Environment, v. 27, p. 1525–1536, doi:10.1111/j.1365-3040.2004.01258.x.
Volkova, V.S., and Kul'kova, I.A., 1996, The Oligocene–early Miocene floral assemblages from western Siberia: Stratigraphy and Geological Correlation, v. 4, p. 496–505.
Volkova, V.S., Kul'kova, I.A., and Fradkina, A.F., 1986, Palynostratigraphy of the non-marine Neogene in North Asia: Review of Palaeobotany and Palynology, v. 48, p. 415–424, doi:10.1016/0034-6667(86)90078-3.
Williams, C.J., Mendell, E.K., Murphy, J., Court, W.M., Johnson, A.H., and Richter, S.L., 2008, Paleoenvironmental reconstruction of a middle Miocene forest from the western Canadian Arctic: Palaeogeography, Palaeoclimatology, Palaeoecology, v. 261, p. 160–176, doi:10.1016/j.palaeo.2008.01.014.
Zachos, J.C., Dickens, G.R., and Zeebe, R.E., 2008, An early Cenozoic perspective on greenhouse warming and carbon-cycle dynamics: Nature, v. 451, p. 279–283, doi:10.1038/nature06588.

Manuscript received 31 October 2016
Revised manuscript received 29 January 2017
Manuscript accepted 31 January 2017

Printed in USA

GSA Data Repository 2017133

The transitional climate of the late Miocene Arctic: Winter-dominated precipitation with high seasonal variability

Brian A. Schubert*, A. Hope Jahren, Sergei P. Davydov, Sophie Warny

*correspondence to: schubert@louisiana.edu

Stratigraphic Context and Palynology Analysis

Fossil wood was collected from the Upper Miocene Khapchansky horizon (Fig. DR1) at the Finish Stream site (modern coordinates: 68.724° N, 161.587° E; paleolatitude: 71–72° N, van Hinsbergen et al., 2015). The Khapchansky horizon contains ferruginous sands with rare pebbles and lenses of silt that have yielded abundant plant detritus and wood fragments, including *Pinus* (evergreen) and mixed deciduous species (Grinenko et al., 1997; Sher et al., 1977). These sampled layers are overlain by the Lower Pliocene Begunovsky horizon (Fig. DR1), which is dominated by very coarse-grained materials, including sand and gravel (pebbles to boulders) (Grinenko et al., 1997). A 50 g subsample of the sediment surrounding the fossil wood within the Upper Miocene Khapchansky horizon was prepared for palynological analyses by Global Geolab Limited (Medicine Hat, Alberta, Canada), and was examined at the LSU Center for Excellence in Palynology (CENEX) using an Olympus BX41 microscope and a 100x oil immersion objective in order to identify pollen, i.e., plant taxa. Examination of the subsamples revealed excellent preservation of the pollen and spore grains, suggesting that they represented *in situ* taxa with minimal transport and reworking. The most abundant palynomorphs were comprised of *Sphagnum* spores and contained little to no *Picea*, *Tsuga*, *Cedrus*, and *Abies* pollen, suggesting a lack of conifer tree species near the site. The dominant tree pollen was from the deciduous genus *Alnus*; an abundance of *Alnus*

with little to no thermophilic angiosperm species (including *Juglans*, *Corylus*, *Quercus*, *Carpinus*, and especially *Fagus*) and no *Taxodiaceae* suggested the site did not span the Miocene Climate Optimum (17-15 Ma) and was consistent with the cooler climate of the late Miocene (Frolov et al., 1989; Grinenko et al., 1997). Therefore, the palynological analysis was consistent with the late Miocene age for the site (11.6 to 5.3 Ma), as suggested by the stratigraphy of the region (Grinenko et al., 1997; Nikitin, 2007).

Stable Carbon Isotope Analysis

All six fossil specimens showed distinctive rings in hand sample with discernable earlywood and latewood anatomy (Fig. DR1); therefore, the direction of growth was known. In total, 36 distinct rings were sampled from the six specimens, resulting in 445 subsamples. In addition, one specimen, Sib13, was measured across two distinct transects in order to assess intra-sample variability. On average, each growth ring was subdivided into 11 increments (mean slice thickness $\pm 1\sigma$: 54 ± 20 μm) to determine bulk $\delta^{13}C$ values (n = 445) across each growth ring.

Eight consecutive growth rings, representing the years A.D. 2005–2012, were identified from within both modern *Pinus* specimens; each of these sixteen rings was then subdivided by hand. On average, each of the modern rings was divided into 16 subsamples for a total of 107 subsamples collected from PINE01 and 148 subsamples collected from PINE02.

Bulk $\delta^{13}C$ values were determined for each intra-ring subsample using a Delta V Advantage Isotope Ratio Mass Spectrometer (Thermo Fisher) coupled to a Thermo Finnigan Elemental Analyzer (Flash EA1112 Series, Bremen, Germany) at the University

of Louisiana at Lafayette and a Eurovector automated elemental analyzer (Eurovector Inc, Milan, Italy) coupled to an Isoprime isotope ratio mass spectrometer (Isoprime, Ltd, Cheadle Hulme, UK) at the University of Hawaii at Mānoa. Isotopic values are reported in δ-notation (‰) against Vienna standards (VPDB). The analytical uncertainty associated with each measurement, assessed using a quality assurance sample that was analyzed as an unknown within each batch run, was < 0.1‰.

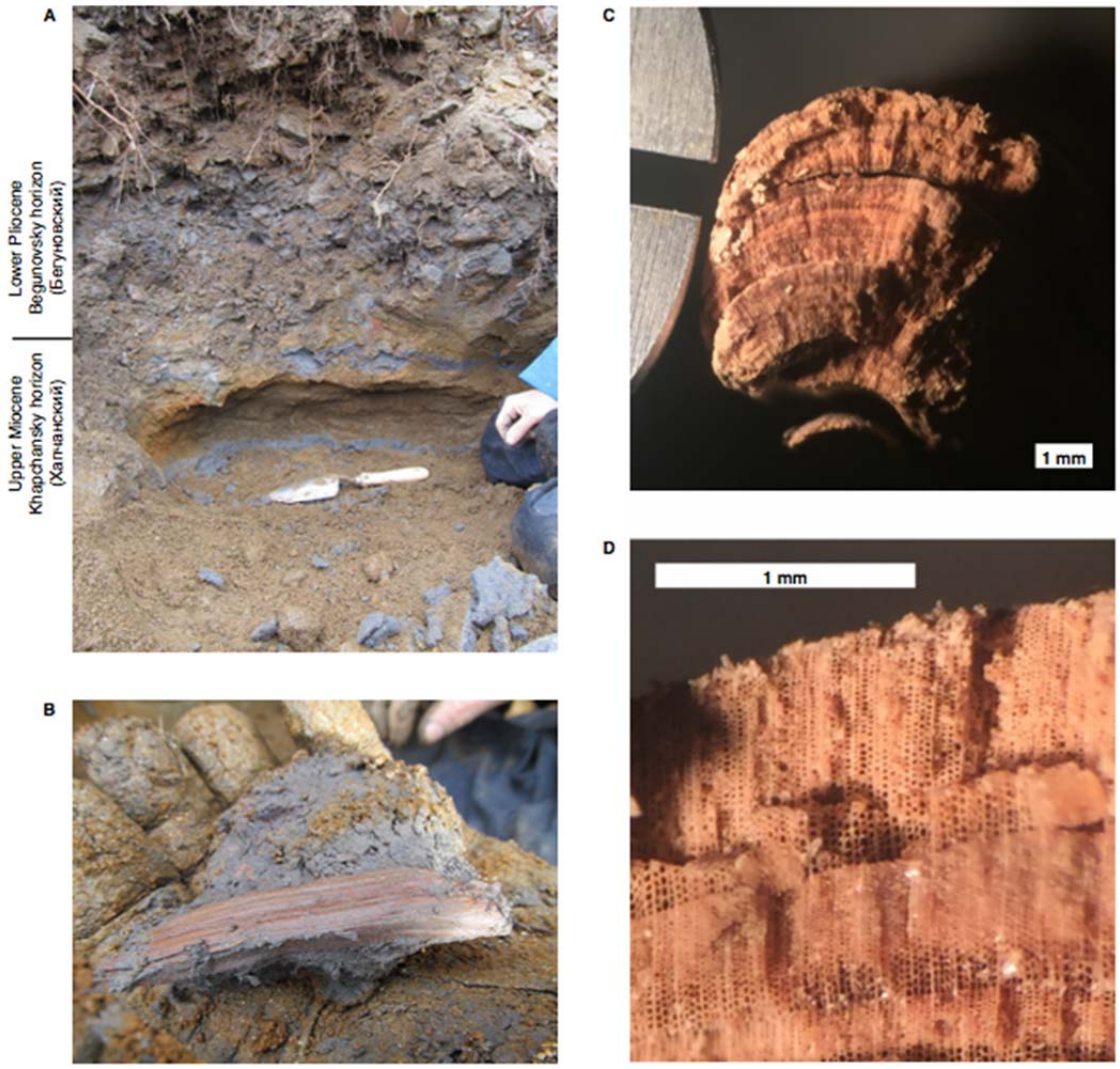

Figure DR1. Fossil wood collected from the Finish Stream site in far northeastern Siberia. (A) Outcrop view showing the coarse grained Lower Pliocene Begunovsky horizon above the fine-grained Upper Miocene Khapchansky horizon. Within the Khapchansky horizon, fossil wood was found in the silty layers (gray), but not within the oxidized sandy lenses. (B) Piece of fossil wood embedded in gray silt. (C) Photograph of sample Sib14-02 showing concentric growth rings. (D) Photograph of sample Sib13 showing well-preserved cellular structure. Because each of the six samples analyzed for this study represented distinct wood fragments with no obvious relationship to each other when discovered in situ, the fossils most likely represented six individuals and that none of the rings sampled represent overlapping time periods. The distinct earlywood and latewood anatomy and concentric curvature of the samples did allow for of the direction of growth (and thus direction of the progression of growing season) to be known.

Figure DR2. Modern *Pinus pumila* sampled for high-resolution intra-ring $\delta^{13}C$ analysis. Field photos of PINE01 (A) and PINE02 (B). (C-D) Cut discs of PINE01 (C) and PINE02 (D) showed annual growth bands. Scale bar is in centimeters.

REFERENCES CITED

Frolov, A. I., Zharikova, L. P., Fradkina, A. F., Grinenko, O. V., Laukhin, S. A., Minyuk, P. S., Savchenko, A. G., and Tumanov, V. R., 1989, Lower-Kolyma trough, The Paleogene and Neogene of the north-eastern USSR: Yakutsk, Academy of Sciences of the USSR: Siberian Branch.

Grinenko, O. V., Sergenko, A. I., and Belolyubsky, I. N., 1997, Stratigraphy of the Paleogene and Neogene sediments of the North East Russia: The Otechestvennaya Geologiya Magazine, v. 8, no. 14-20 [in Russian].

Nikitin, V. P., 2007, Paleogene and Neogene strata in Northeastern Asia: Paleocarpological background: Russian Geology and Geophysics, v. 48, p. 675-682.

Sher, A. V., Giterman, R. E., Zazhigin, V. S., and Kiselyov, S. V., 1977, New data on the late Cenozoic deposits of the Kolyma lowland: Academy of Sciences of the U.S.S.R., Isvestiya, Series Geologie, p. 69-83 [in Russian].

van Hinsbergen, D. J. J., de Groot, L. V., van Schaik, S. J., Spakman, W., Bijl, P. K., Sluijs, A., Langereis, C. G., and Brinkhuis, H., 2015, A paleolatitude calculator for paleoclimate studies (model version 2.0): PLOS ONE, v. 10, no. 6, p. e0126946.